Journal of Applied Sciences

ISSN 1812-5654

science alert

ANSInet
an open access publisher
http://ansinet.com

Journal of Applied Sciences 8 (3): 480-488, 2008
ISSN 1812-5654

Improvement of Remote Sensing Techniques in TPW Assessment Using Radiosonde Data

[1]M.R. Mobasheri, [2]S.M. Purbagher Kordi, [3]M. Farajzadeh and [4]A. Sadeghi Naeini
[1]Department of Remote Sensing, KNToosi University of Technology,
Mirdamad Cross, Valiasr Ave., P.O. Box 15875-4416, Post Code 1996715433, Tehran, Iran
[2]I.R. of Iran Meteorological Organization, Tehran, Iran
[3]Department of Remote Sensing and GIS, Tarbiat Modares University, Tehran, Iran
[4]Iran Space Agency, Tehran, Iran

Abstract: A great amount of efforts have so far been devoted to the global determination of Total Precipitable Water (TPW) but little work is directed toward the regional assessment of TPW using remote sensing techniques. To increase the level of confidence in TPW assessment in the local to regional scale using satellite imageries, a simultaneous *in situ* measurement by radiosonde and satellite over passing were carried out. The results show a high correlation (0.93) between radiosondes data and the ratio of the two absorption band (narrow band to a wide band). This in MODIS sensor is the ratio of channel 18 to channel 19. It is found that the application of different algorithms via classification of the atmosphere by its water vapor content and definition of threshold values for TPW, may not work in the confined regions such as Tehran capital city of Iran. The result of this study is presented through a conversion equation like TPW (Real) = a.$TPW_{18/19}$ + b. More work is required to evaluate applicability of this equation for different seasons and different states of the atmosphere.

Key words: Remote sensing, water vapor, radiosonde, algorithm

INTRODUCTION

Atmospheric water vapor is a key climatological variable because of its capacity to drive energy exchanges between the ocean and the atmosphere and within the atmosphere by releasing latent heat. Moreover, of all atmospheric gases, water vapor exhibits the largest spatial and temporal variations and has the potential to drive a large positive feedback in global warming scenario (Rind *et al*., 1991). Global determination of the Total Precipitable Water vapor (TPW) distribution is important in boosting the understanding of the physical processes such as hydrological cycle, biospheric-atmospheric interactions, the energy balance and for monitoring climate change due to the greenhouse gases effects (Menzel *et al*., 2002).

On the other hand, the complex interaction between water vapor, aerosol and clouds renders quantification of water vapor feedback without further systematic measurements of water vapor, aerosol and clouds very difficult (Menzel *et al*., 2003). It is also of particular importance to monitor seasonal and annual changes in the precipitable water on local to regional scales in order to monitor drought conditions and decertification processes as well as floods.

Accurate global mapping of atmospheric water vapor is an important objective of the global energy and water cycle assessment. However, the local scale assessment can assist in improved weather forecasting as well as nowcasting (Mobasheri, 2004).

The sparse location of ground monitoring stations, especially in arid areas, merits the need for an accurate remote sensing technique that can provide water vapor information on a daily basis with an adequate spatial resolution (e.g., 1-5 km from MODIS).

Currently available infrared sounder sensors are capable of retrieving water vapor profiles as a byproduct of remote sensing of the atmospheric temperature profiles (Mobasheri, 2007). The derived water vapor profile depends in part on the initial guess for the temperature and moisture profiles assumed in the inversion equations and consequently being sensitive to these initial profiles especially close to the surface region (Menzel *et al*., 2003).

Kleespies and McMillin (1990) developed a split window technique that utilizes temperature variation in a heterogeneous terrain. They found a correlation better

Corresponding Author: M.R. Mobasheri, Department of Remote Sensing, KNToosi University of Technology, Mirdamad Cross, Valiasr Ave., P.O. Box 15875-4416, Post Code 1996715433, Tehran, Iran
Tel:+98 9121226630 Fax: +98 2188786213

than 0.7 between the *in situ* and retrieved water vapor. In arid regions where the difference between the surface and the boundary layer temperature is large (e.g., central region of Iran during the afternoon), a high correlation was found between the apparent temperature difference in the 11 and 12 μm bands and total precipitable water.

A technique based on differential absorption of water vapor was suggested by Frouin *et al.* (1990) and Frouin and Middleton (1990) where in this technique, two water vapor channels centered at the same wavelength of 0.94 μm but having different band widths (of 17 and 45 nm) were used. These channels show different sensitivities to the variation in the amount of atmospheric water vapor but no (or small) sensitivity to the surface reflectance. Consequently a ratio of the radiances measured in these two channels could almost be independent of the surface reflectance. Also the ratio of a water vapor absorption band to a nearby non-absorbing band can be calibrated for TPW determination (Chylek *et al*., 2003). This is the objective of this research.

MATERIALS AND METHODS

Methodology of this work is based on the regression between two TPW values estimated through Remote Sensing and Radiosonde techniques. From theoretical points of view, it follows that if the apparent surface temperature (not corrected for the emissivity effects) is about equal to the mean temperature of the boundary layer, where usually most of the water vapor resides, the emitted radiance in infrared and microwave region will not be sensitive to the boundary layer water vapor (Kaufman and Gao, 1992). In this case, any emission in the IR or microwave from the surface will be absorbed by water vapor in the boundary layer and will be remitted from this boundary layer, thus having little effect on the upwelling radiance (Mobasheri, 2007).

In this research, it is decided to base our work on the use of an optical technique offered by Kaufman and Gao (1992) that utilizes the solar radiation reflected by the surface for remote sensing of water vapor from the Moderate Resolution Imaging Spectrometer (MODIS) onboard of Earth Observing platform Terra and Radiosonde technique simultaneously. Although the procedure is the same but the selected technique is different. The technique is applicable to the cloud free images acquired over land.

Although MODIS instrument has a low spatial resolution (1 km), but on the other hand this deficiency make it capable of having a global coverage within a period of 2 to 3 days.

Since water vapor has a high spatial and temporal variability; therefore, a revisiting time of 2 to 3 days make MODIS products ideal for the study of the biosphere-atmosphere interaction, its relation to global change and producing global maps of water vapor distribution. In this regards, two channels of MODIS-N specifically designed for monitoring the global distribution of water vapor over the land in cloud-free conditions, were selected.

The technique is based on detection of the absorption of solar radiation by water vapor as it is transmits down to the surface and up to the sensor through the atmosphere.

Ground-based transmission measurement of water vapor by sunphotometers from in and around the near IR absorption bands has been reported (Menzel *et al*., 2002; Chylek *et al*., 2003). These measurements were carried out via transmitted sun light in a channel that corresponds to the water vapor absorption (0.94 μm) as well as nearby channels in atmospheric windows (0.87 and 1.03 μm).

A comparison between the reflected solar radiation in the absorbing bands and the reflected solar radiation in nonabsorbing bands can quantify the total vertical amount of water vapor. The main uncertainty in the determination of water vapor comes from evaluation of the surface reflection for heterogeneous surfaces in the absorption band (Kaufman and Gao, 1992). In these cases, more non-absorbing (window) channels are required to "predict" the surface reflectance in the water absorption channel and consequently less accuracy can be expected.

The good MODIS water vapor spectrum offers a variety of possibilities, from a strong absorption in a narrow channel around 0.935 μm (used for detection of water vapor in clouds), to more moderate absorption around 0.95-0.97 μm and to a weaker absorption around 0.91 μm.

Kaufman and Gao (1992) based their technique of remote sensing of water vapor on a ratio of absorbing to non-absorbing channels (e.g., a ratio of the measured radiation at 0.94 μm to that of 0.86 μm), or alternatively on a ratio of a strongly absorbing channel (e.g., a narrow channel centered at 0.94 μm) to that of a moderately absorbing channel (e.g., a wide channel centered at 0.94 μm) where the latter technique, proposed by Frouin *et al.* (1990) significantly reduces the effect of surface reflectance on the channel ratio. Of course this also significantly reduces the sensitivity of the channel ratio to water vapor. Kaufman and Gao (1992) then related this ratio to the total precipitable water W through some empirical relationship of the form:

$$T_w(\rho_{ab}/\rho_{non-ab}) = \exp(\alpha - \beta\sqrt{W}) \quad (1)$$

based on reflectance values of different surfaces in absorbing channels (ρ_{ab}) and non-absorbing channels

(ρ_{non-ab}). α and β are coefficient that can be determined through some in situ measurements. For a mixture of all surfaces, values of $\alpha = 0.020$ and $\beta = 0.651$ can be used (Kaufman and Gao, 1992).

T_w can also be defined as a function of the precipitable water vapor along the optical path, W* which is related to the total precipitable water vapor W by Kaufman and Gao (1992):

$$W^* = W(1/\cos\theta + 1/\cos\theta_o) \quad (2)$$

$$T_w(\rho_{ab}/\rho_{non-ab}) = \exp(\alpha - \beta\sqrt{w^*}) \quad (3)$$

here θ and θ_o are view zenith angle and solar zenith angle, respectively. The coefficients for the best fit to T_w, as a function of W* for the MODIS water vapor channels suggested by Kaufman and Gao (1992) is given in Table 1.

Three different band ratios can be assigned to T_w for three different states of the atmospheric water vapor contents:

Dry atmosphere: In this case, the reflectance ratio of channel 18 to channel 2 as a function of the amount of water vapor is recommended. In the case of very small water vapor content (W < 0.5 cm water), the main error in the remote sensing technique may result from uncertainty in the spectral surface reflectance. To minimize this effect, a ratio of the narrow channel of 18 to the wide channel 19 can be used. Then T_w can be found from:

$$T_w = \rho_{0.931-0.941}/\rho_{0.915-0.965} = \exp(\alpha - \beta\sqrt{W^*}) \quad (4)$$

Low to moderate water vapor: For TPW of around 2 cm in nadir or even less than 2 cm in off-nadir viewing angle, ratio of channel 19 to channel 2 is suggested (Kaufman and Gao, 1992).

$$T_w = \rho_{0.915-0.965}/\rho_{0.841-0.876} = \exp(\alpha - \beta\sqrt{W^*}) \quad (5)$$

Humid atmosphere: For total precipitable water vapor amount larger than 4 cm in nadir view condition or even less than this value but for slant view and illumination conditions, the strong absorption in the proposed 0.915-0.965 μm channel may partially saturate, resulting in lower sensitivity to water vapor (Table 2). In this case, a water vapor absorption band in a spectral range corresponding to lower absorption i.e., 0.890-0.920 μm for remote sensing of water vapor in humid conditions is preferred (Kaufman and Gao, 1992). This band is located in spectral region with minimum values of change in T_w.

$$T_w = \rho_{0.890-0.920}/\rho_{0.841-0.876} = \exp(\alpha - \beta\sqrt{W^*}) \quad (6)$$

Table 2 shows the particulars of three water vapor absorption MODIS bands of 17, 18 and 19.

TPW calculation using radiosonde data: Radiosonde is a telemetric system that can measure atmospheric parameters such as air temperature, pressure and humidity as it ascends through the air. Then this system transmits the collected data to the ground stations. Moreover, wind speed and direction will also be measured using balloon's speed and direction relative to the surface below.

To calculate TPW using radiosonde data the following steps were adopted:

Step 1: Calculation of water vapor partial pressure e: To calculate vapor partial pressure e which is equal to the saturated partial pressure at dew point temperature, we used the dew point temperature and the equation offered by Rogers and Yau (1996):

Table 1: Values of α and β for different absorbing and non-absorbing band and for two viewing angles of nadir ($\theta = 0, \theta_o = 40$) and off-nadir ($\theta = 60, \theta_o = 60$) (Kaufman and Gao, 1992)

View	Absorbing band	Eq. MODIS channel	Non-absorbing band	Eq. MODIS channel	α	β
Nadir	0.890-0.920	17	0.841-0.876	2	0.016	0.209
Off-nadir	0.890-0.920	17	0.841-0.876	2	-0.003	0.181
Nadir	0.931-0.941	18	0.841-0.876	2	0.043	0.760
Off-nadir	0.931-0.941	18	0.841-0.876	2	-0.110	0.537
Nadir	0.931-0.941	18	0.915-0.965	19	0.029	0.332
Nadir	0.915-0.965	19	0.841-0.876	2	0.036	0.426
Off-nadir	0.915-0.965	19	0.841-0.876	2	-0.024	0.342

Table 2: Characteristics of the absorption bands used in this study

Application	Signal to noise	Band width (nm)	Wavelength (nm)	Channel No.
Very humid atmosphere: Weak water vapor absorption	167	30	920-890	17
Dry atmosphere: Strong water vapor absorption	57	10	941-931	18
No cloud, ordinary atmosphere: Moderate water vapor absorption	250	50	965-915	19

$$e = e_s(T_d) = 6.11\exp[\frac{L_v}{R_v}(\frac{1}{273.15} - \frac{1}{T_d})] \quad (7)$$

Where:

T_d = Dew point temperature
$L_v = 2.5\times10^6$ (j kg^{-1}) = Latent heat of evaporation
$R_v = 461.5$ (j k^{-1} kg^{-1}) = Universal gas constant

Step 2: Specific humidity: Specific humidity can be calculated using Eq. 8 suggested by Hurly (1994).

$$q = q(T_d) = \frac{0.622e_s(T_d)}{[P - 0.378e_s(T_d)]} \quad (8)$$

Where, q would be in g kg^{-1}. T_d and P are from nearby weather station and $e_s(T_d)$ from Eq. 1 in step 1.

Step 3. Calculation of total water vapor: The TPW was worked out using all calculated q values at different level with pressure P and equation offered by Carlson *et al*. (1991):

$$TPW = -\frac{1}{\rho_w g_m}\int_{P_0}^{0} q.dP \quad (9)$$

Where:

ρ_w = 1000 kg m^{-3} is water density
q = Specific humidity in g kg^{-1} and TPW in mm
g_m = Mean acceleration due to gravity in m s^{-2} which varies with latitude and height

Site and data selection: Temperature, pressure and dew points are parameters that are collected and transmitted to the surface by radiosonde sensors directly. A relatively complete bank of radiosonde data are in access at the Wyoming University site as well as Iran Meteorological Organization. These data are being collected on a routine basis two times a day on the synoptic hours, i.e., 0000Z and 1200Z (GMT). The selected site for this work was Mehrabad Airport synoptic station located in Southern part of Tehran capital city of Iran where the location is shown in Fig. 1. This station is located at 51°, 21 E and 35°, 41'N at an altitude of 1191 m from sea level. The index of this station is OIII and its number is 40754.

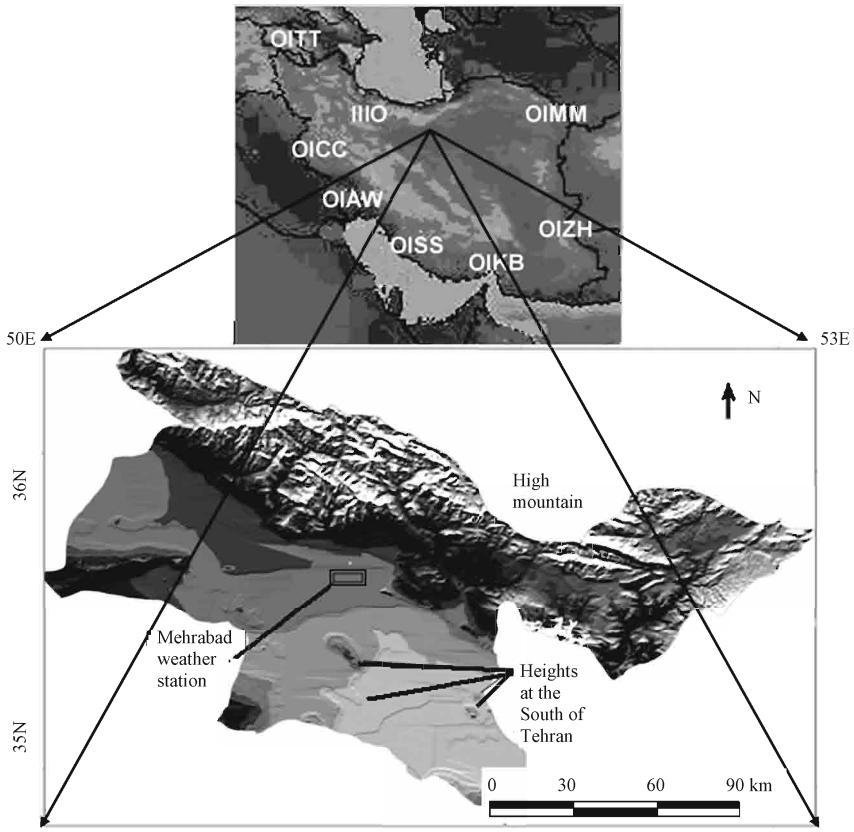

Fig. 1: A DEM of the Mehrabad synoptic station region located at south of capital city of Tehran southern slopes of Alborz Mountains. White codes are for those stations where radiosondes collect data on a routine basis

MODIS images are only available from 1999. To select proper data, we first selected cloud free MODIS images and then selected the radiosonde data as close as possible to the satellite acquisition time. To carry out weather analysis for the time of study, the thermodynamic graphs such as Stuve or Skew-T were used. In these graphs, temperature, pressure and dew point profiles as well as condensation temperature and pressure were studied.

This helped extraction of information regarding atmospheric stability as well as the possibility of the presence of small patches of clouds that can not be detected in the low resolution MODIS images, otherwise. Presence of small patches of clouds within a pixel increases the uncertainty of TPW assessment using satellite imageries (Jeffery and Austin, 2003).

Geometrical processing on MODIS images were carried out by Iran Space Agency. Radiometric correction by pixel to pixel method was carried out using IMMAP software and parameters retrieved from image header file. Finally using Scan Magic software, geometrical corrections based on Lambertian system with elliptical base of WGS84 was done applying nearest neighbourhood method and parameters retrieved from image header file. Finally using Scan Magic software, geometrical corrections based on Lambertian system with elliptical base of WGS84 was done applying nearest neighbourhood method.

Image selection: Upon thorough investigation and analysis of weather condition, four MODIS images were selected particulars of which are shown in Table 3.

Weather analysis: Application of one TPW retrieving algorithm for two images with similar acquisition time (from seasonal point of view) may result in completely different values partly due to weather condition at the satellite passing time. Since water vapor retrieving algorithm can only be applied in the cloudless sky, then the weather condition (cloudiness, water vapor, presence of a front) around satellite passing time need to be investigated using synoptic data. This may increase our confidence about the retrieved TPW values.

To avoid ambiguities resulting from weather conditions, parameters such as wind speed and direction, dry and wet bulb temperature, dew point, soil temperature, relative humidity and partial vapor pressure were investigated prior to the image selection in this work. Also Stuve graphs at the vicinity of satellite passing time were plotted using Radiosonde data. Through these thorough investigations, finally four images were selected (Table 3) where details of their Stuve graphs are shown in Fig. 2-5.

Table 3: Sun and Sensor zenith angles along with conversion coefficients for four MODIS images

Acquisition date	Band No.	Scale	Offset	Sun zenith	Sensor zenith
May 26, 02	2	34111	972.316	66.17	13.30
	17	233312	17.660	17.66	30.13
	18	338274	316.972	17.66	30.13
	19	248247	316.972	17.66	30.13
May 26, 03	2	340200	316.972	22.42	27.05
	17	235272	316.972	22.42	27.05
	18	338100	316.972	22.42	27.05
	19	248824	316.972	22.42	27.05
Sep 15, 02	2	307884	316.972	34.22	29.76
	17	216424	316.972	34.22	29.76
	18	343334	316.972	34.22	29.76
	19	252829	316.972	34.22	29.76
Sep 17, 04	2	331413	316.972	37.96	27.40
	17	231434	316.972	37.96	27.40
	18	332584	316.972	37.96	27.40
	19	244764	316.972	37.96	27.40

Since MODIS passing time is 7:30 (GMT) then any profiles at the satellite passing time must be interpolated from the two Radiosonde profiles of 00Z and 12Z. These interpolated profiles are only valid when the two profiles of 00Z and 12Z show similar shape and behavior. Figure 2 shows that almost in all four different dates, except at the region close to the surface, the temperature profiles at 12Z do not deviate much from those of 00Z, although the dew point profiles in three of these dates at 00Z and 12Z are notably different. This means that the interpolation of temperature profile for the time of satellite passage would be acceptable. On the other hand the abrupt deviation of dew point profiles at any altitude may represent the occurrence of change in water vapor content at that altitude. This could be due to the condensation, if dew point decreases (possible cloud formation at 400 mb for Sep 15th and May 26th, 2002) or entrance of water vapor to that altitude brought by possible fronts and/or wind as in Sep15 and May 26, 2002 plots. To clarify this, one may use other profiles such as water vapor density (Fig. 3), wind speed (Fig. 4) and wind direction (Fig. 5).

As an illustration of the analysis, the anomaly in dew point profile of Sep15, 2002 and May 26, 2002 at 400 mb level was due to a decrease in density (absolute humidity) of water vapor as can be seen in Fig. 3 by high westerly winds (Fig. 4, 5). However this anomaly can not cause any problem in TPW assessment due to the low water vapor content of the atmosphere at this height (Fig. 3).

The anomaly of dew point profiles at around 700 mb in Fig. 2 show a decrease for Sep 15th and May 26th, 2002 and slight (ignorable) increase at the same altitude for Sep 17, 2004 and May 26, 2003 between 00Z and 12Z. Figure 3 shows abrupt decrease in absolute humidity on Sep. 15th and May 26th, 2002 for this time interval while wind speed is much higher for May 26, 2002 compare to

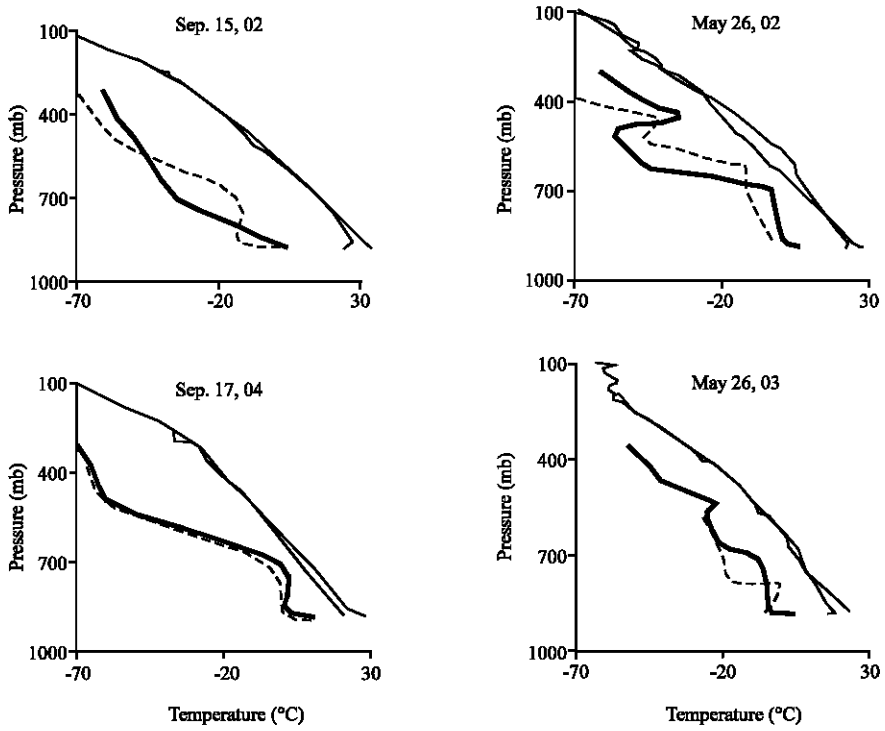

Fig. 2: Dewpoint (bold lines) and temperature profiles (non-bold lines) at 00Z (dashed) and 12Z (solid) in four different satellite passing date

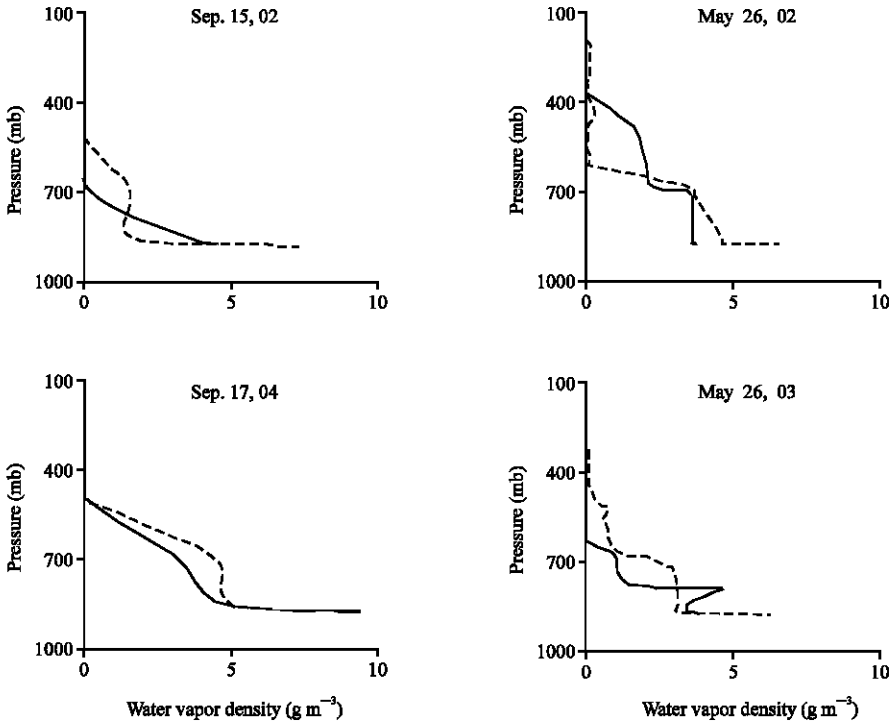

Fig. 3: Water vapor density (absolute humidity) at 00Z (dashed) and 12Z (solid) in four different satellite passing date

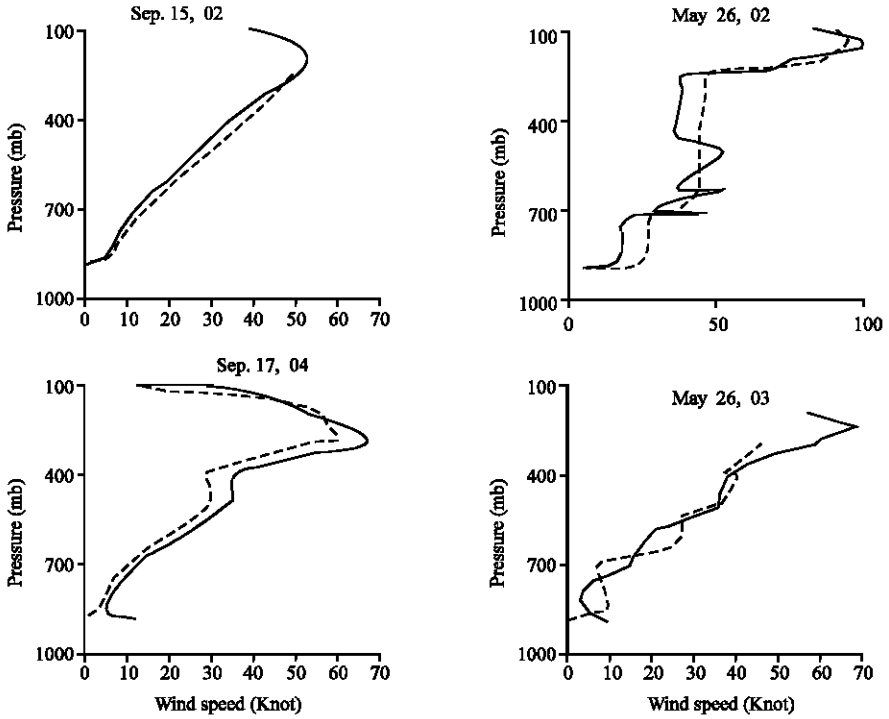

Fig. 4: Wind speed profile at 00Z (dashed) and 12Z (solid) in four different satellite passing date

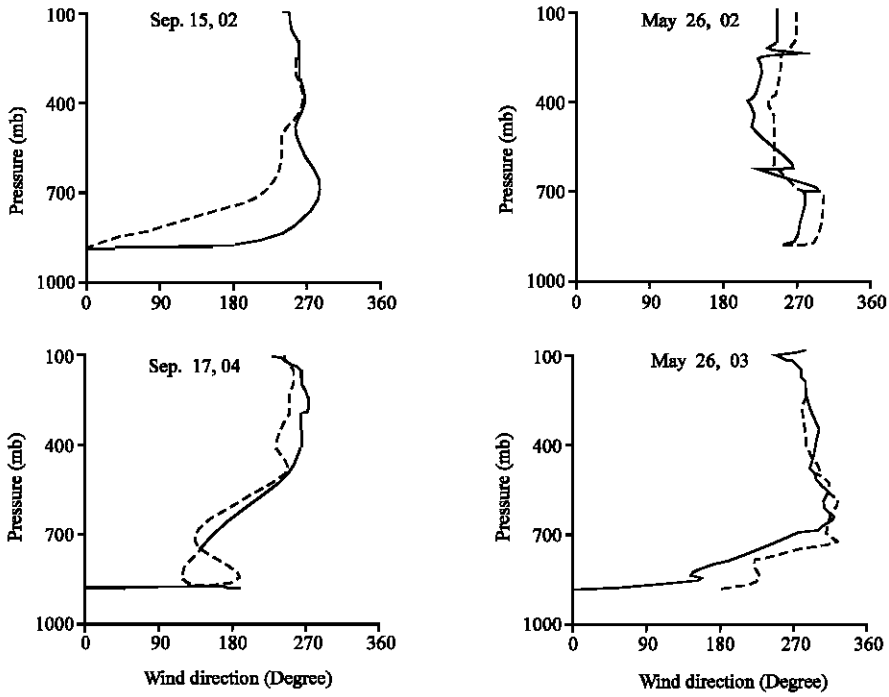

Fig. 5: Wind direction at different altitudes (pressures) for 00Z (dashed) and 12Z (solid) in four different satellite passing date

Sep. 15th. The decrease in water vapor content could be mostly due to the southerly to westerly wind blowing during this time interval.

Due to the fact that the great portion of the atmospheric water vapor content resides close to the surface and upon the above analysis, day Sep. 15, 2002 has the driest atmosphere and Sep. 17, 2004 has the wettest atmosphere compare to the other two days where the humidity of the atmosphere is more moderate. Between these two, May 26, 2002 seems more humid than May 26, 2003. This also can be concluded from absolute humidity profiles in Fig. 3. Since in all these profiles, water vapor abruptly decreases with height, no condensation is likely to happen above 500 mb and consequently there is no chance for cloud formation to occur. On the other hand according to the classification mentioned in previous section (Kaufman and Gao, 1992) all of these four states of the atmosphere can be classified in Humid atmosphere and according to (Kaufman and Gao, 1992) the ratio of band 17 to band 2 must be applied for TPW assessment.

RESULTS AND DISCUSSION

Applying Eq. 8-10 to radiosonde data and Eq. 4- 6 to MODIS reflectance images resulted in TPWs which are shown in Table 4. As can be seen in Table 4, none of the four days Sep. 15, 2002; May 26, 2002; May 26, 2003 and Sep. 17, 2004 have possessed the conditions mentioned for dry atmosphere but as a comparison, as mentioned before Sep. 15, 2002 has the driest and Sep. 17, 2004 has the wettest atmosphere among these four days.

According to Kaufman and Gao, (1992) classification reflectance ratio of band 17 to band 2 was expected to be the most suitable one for TPW assessment in all these four atmospheric states, but in practice the worst correlation between Radiosonde and satellite TPW was found with this ratio (Table 5).

The possible explanation for this could be the special geography of the region where all of the atmospheric water vapor contents are trapped in the height between 1200 to 3000 m and it is not distributed logarithmically in height as is expected for a normal atmosphere. A regression between satellite derived TPW with the Radiosonde TPW were ran using least square method results of which is shown in Table 5.

In Table 5, the poorest correlation is for 17/2 (0.00) and the best one is for 18/19 (0.93). It is believed that the ratio of the two water vapor channels centered at the same wavelength (such as MODIS channel 19 (0.94 μm) and channel 18 (0.936 μm) having different band widths (50 and 10 nm, respectively) may renders the effects of surface reflectance on the results, minimum. This is because these channels show different sensitivity to the variation of the amount of atmospheric water vapor but no (or small) sensitivity to the surface reflectance (Frouin *et al*., 1990; Frouin and Middleton, 1990). Consequently a ratio of the reflectance measured in these two channels could almost be independent of the surface reflectance.

This might be the case for Mehrabad urban region where variety of surface covers is present in each pixel. The second suitable ratio is 18/2 (0.84) that is suggested for moderate atmospheric humidity content by Kaufman and Gao, (1992). This could be suitable for the region because of the geometry where the Alborz Mountains with height of more than 4000 m have surrounded the region.

Figure 6 shows the regression between shaded boxes in Table 5 and radiosonde TPW data with a correlation coefficient of 0.81 where we call it Combination Method. Although the correlation coefficient is a little lower in Combination Method compare to 18/19 ratio but since we are using three band ratios (including 18/19 which minimizes the surface reflectance effects) rather than one band ratio (18/19), the uncertainties due to the threshold values suggested by Kaufman and Gao (1992) might decrease. However in practice Combination Method has its own difficulties and needs more *in situ* measurement to determine the coefficients such as a, b, c and d in the following equation:

$$TPW(Radiosonde) = a.TPW_{18/19} + b.TPW_{19/2} + c.TPW_{18/2} + d \quad (10)$$

Of course these coefficients may depend on the region's topography and/or geography where these authors are working on it.

Then the suggested model for the region under study would be of the form;

Table 4: Results of calculated TPW using radiosonde and satellite data. Shaded data are selected for regression. Shaded boxes are for a combination of band ratios

Satellite passing date		15.09.2002	26.05.2002	26.05.2003	17.09.2004
Radiosonde Measured TPW (mm)		5.37	9.78	7.27	13.48
Satellite Predicted TPW for Mehrabad Airport region (mm)	17 to 2	4.95	0.56	4.69	5.51
	18 to 2	10.00	12.56	8.38	22.98
	19 to 2	4.90	5.11	6.58	12.57
	18 to 19	5.64	13.43	9.54	15.67

Table 5: Regression coefficients between satellite and radiosonde derived TPWs

J/I = a*Radiosonde + b	a	b	R^2
17/ 2	-0.015	4.070	0.00
18/2	1.717	-1.930	0.84
19/2	0.864	-0.469	0.71
18/19	1.216	0.156	0.93

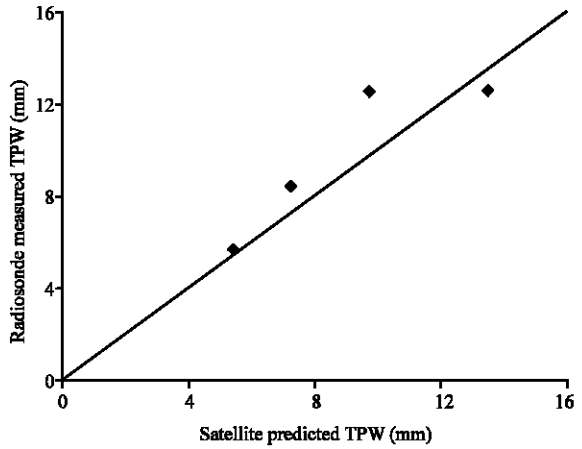

Fig. 6: Regression between radiosonde estimated TPW and satellite derived TPW (shaded boxes in Table 5), $R^2 = 0.81$

$$TPW(Real) = a.TPW_{8/19} + b \quad a = 1.216,\ b = 0.156,\ R^2 = 0.93 \tag{11}$$

This may increase the accuracy of satellite TPW assessment up to 20% which is important for the forecasting of natural disasters such as flood in mountainous regions like Tehran.

ACKNOWLEDGMENTS

We would like to acknowledge valuable assistance of Mr. Yusef Rezaie in image processing and also helpful cooperation of Iran Space Agency in providing MODIS images for this research. Also we would like to appreciate I.R. of Iran Meteorological Organization for providing Radiosonde and synoptic data. Finally this research has been funded by Water Resource Management of I.R. Iran's Energy Ministry and we appreciate their thoughtful assistance.

REFERENCES

Carlson, T.N., E.M. Perry and T.J. Schmugge, 1990. Remote estimation of soil moisture availability and fractional vegetation cover for agricultural fields. Agric. For. Meteorol., 52: 45- 69.

Chylek, P., C.C. Borel, W. Clodius, P.A. Pope and A.P. Rodger, 2003. Satellite based columnar water vapor retrieval with the multi-spectral thermal imager (MTI). IEEE Trans. Geosci. Remote Sen., (Accepted).

Frouin, R., P.Y. Deschamps and P. Lecomte, 1990. Determination from space of atmospheric total water vapor amounts by differential absorption near 940 nm: Theory and airborne verification. J. Applied Meteorol., 29: 448-460.

Frouin, R. and E. Middleton, 1990. A differential absorption technique to estimate atmospheric total water vapor amounts. In: Proceeding of the Symposium on the first IS.SCP Field Experiment, Feb. 7-9, Anaheim, CA 135-139.

Hurly, P.J., 1994. A lagrangian partic/puff approach for plume dispersion modeling. J. Applied Meteor., 40: 5-15.

Jeffery, C.A. and P.H. Austin, 2003. Unified treatment of thermodynamic and optical variability in a simple model of unresolved low clouds. J. Atmos. Sci., 60: 1621-1631.

Kaufman, Y.J. and B.C. Gao, 1992. Remote sensing of water vapor in the near IR from EOS/MODIS. IEEE Trans. Geosci. Remote Sens., 30: 871-884.

Kleespies, T.J. and L.M. McMillin, 1990. Retrieval of precipitable water from observations in the split window over varying surface temperatures. J. Applied Meteorol., 29: 851-862.

Menzel, W.P., S.W. Seemann, J. Li and L.E. Gumley, 2002. Modis atmospheric profile retrieval algorithm theoretical basis document. University of Wisconsin-Madison. Version 6, pp: 1-39.

Menzel, W.P., S.W. Seemann, J. Li and L.E. Gumley, 2003. Operational retrieval of atmospheric temperature, moisture and ozone from MODIS infrared radiances. J. Applied Meteorol., 42: 1072-1091.

Mobasheri, M.R., 2004. An advanced international course in satellite meteorology in regional meteorological training center (Rmtc). Under World Meteorological Organization (WMO), 12-23 Jun, 2004, Tehran, Iran.

Mobasheri, M.R., 2007. Fundamental of Physics in Remote Sensing and Satellite Technology, Farsi (Ed.). KNToosi University of Technology Publication, pp: 318.

Rind, D., E.W. Chiou, W. Chu, J. Larsen, S. Oltmans, J. Lerner, M.P. McCormick and L. MacMaster, 1991. Positive water vapor feedback in climate models confirmed by satellite data. Nature, 349: 500-503.

Rogers, R.R. and M.K. Yau, 1996. A Short Course in Cloud Physics, Pergamon Press.